PROCEEDINGS OF SCIENCE

Measurements of Drell–Yan processes with ATLAS

Émilien Chapon[a,*] **for the ATLAS Collaboration**

[a] *IRFU, CEA, Université Paris-Saclay, Gif-sur-Yvette, France*

E-mail: emilien.chapon@cern.ch

Precision measurements of Drell–Yan processes, including on-shell and off-shell W- and Z-boson production, offer key input to improve the understanding of QCD and the accuracy of PDFs. In addition, Drell–Yan measurements are instrumental for precision measurements of fundamental electroweak parameters, such as the W boson mass measurement. This talk summarizes recent results from ATLAS on this topic.

The European Physical Society Conference on High Energy Physics (EPS-HEP2025)
7-11 July 2025
Marseille, France

*Speaker

ISSN 1824-8039. Published by SISSA Medialab.

PoS(EPS-HEP2025)288

1. Introduction

The Drell–Yan process, the production of a pair of leptons from quark–antiquark annihilation, is a clean and well-understood process, both experimentally and theoretically. The production cross sections, both for the charged and neutral Drell–Yan processes, are among the largest at the LHC. At the same time, they give a clean experimental signature, including isolated leptons, and these measurements typically feature low backgrounds. Very precise perturbative calculations are available, up to the fourth order in the strong coupling constant (second order for electroweak corrections) and fourth order in the leading logarithm expansion.

As a consequence, Drell–Yan measurements provide precision checks of the Standard Model (SM). First, fundamental parameters of the SM, such as the W-boson mass or the weak mixing angle, can be measured up to very high precision. Perturbative quantum chromodynamics (pQCD) calculations can also be validated against the Drell–Yan data. Finally, they also give access to many non-perturbative QCD effects, such as the parton distribution functions, or the description of the low transverse momentum region using q_{T} resummation or parton shower. As a consequence, Drell–Yan measurements are also instrumental to searches for physics beyond the SM, either as a background to direct searches or in parameterising any deviations to the SM in the framework of effective field theories.

In this contribution, three recent measurements from the ATLAS experiment [1] are reviewed: W cross sections with low pile-up data [2], charged-current Drell–Yan at high transverse mass [3], and high-mass Drell–Yan in the $\tau\tau$ final state [4].

2. W cross sections with low pile-up data

W cross sections are sensitive probes of pQCD calculations, as well as parton distribution functions (PDFs). In particular, there is a strong correlation between the boson rapidity y and the longitudinal momentum fraction of the struck parton in the proton (also known as Bjorken x): $x \propto \frac{M_W e^{\pm y}}{\sqrt{s}}$. In the measurement of W boson production cross sections using low pile-up data [2], cross sections are measured as functions of the charged lepton transverse momentum p_{T} and pseudorapidity η, in one or two dimensions.

This measurement uses low pile-up data recorded in 2017 and 2018 at centre-of-mass energies of $\sqrt{s} = 5.02$ and 13 TeV, providing excellent experimental conditions, leading to small systematic uncertainties. This dataset has also been used in another recent ATLAS publication, the precise measurement of W and Z boson transverse-momentum-dependent cross sections [5], which will not be discussed here.

Both the electron and muon channels are used, while $W \to \tau\nu$ is treated as background. The fiducial region is defined as follows, using Born-level kinematics: charged lepton $p_{\mathrm{T}}^{\ell} > 25\,\mathrm{GeV}$, $|\eta| < 2.5$, $m_{\mathrm{T}}^{W} > 50\,\mathrm{GeV}$, and $p_{\mathrm{T}}^{\nu} > 25\,\mathrm{GeV}$. Results are unfolded for detector effects using iterative Bayesian unfolding. The dominant systematic uncertainty (up to 5%) arises from the choice of MC generator for $W^{\pm}$ production, and is estimated by comparing Sherpa with the nominal Powheg+Pythia, which use different assumptions and models for their predictions, in particular regarding the underlying event.

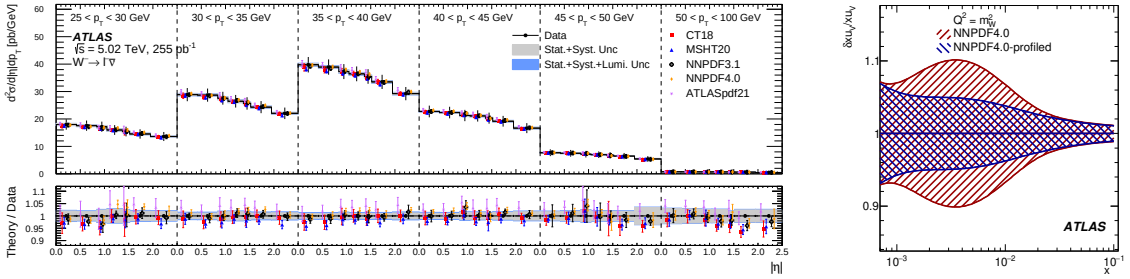

Figure 1: Left: unfolded $W^- \to \ell^- \bar{\nu}$ cross section as functions of the lepton p_{T} and η, compared to predictions using different PDFs. Right: expected impact of the measured cross sections on the valence u-quark PDF, as estimated from a profiling of NNPDF4.0. Figures from Ref. [2].

The measured cross sections are compared to predictions by DYTurbo at next-to-next-to-leading order accuracy in QCD ($\mathrm{NNLO_{QCD}}$) and next-to-next-to-leading logarithm (NNLL), and a good agreement is found overall, except in the high p_{T} tail. When compared with predictions using different PDFs (at NNLO), better description are found by NNPDF3.1 and NNPDF4.0 compared to CT18, MSHT20, and ATLASpdf21. As can be seen from Figure 1 (left), the measurement is more precise than the predictions, especially in the case of the charge asymmetry (not shown here), which hints to the potential for additional constraints on the PDFs.

In order to quantify this potential, PDFs are profiled using the xFitter software. Grids have been computed using MadGraph5_aMC@NLO, with NNLO k-factors obtained from DYTurbo. Figure 1 (right) shows that a sizeable reduction of uncertainties can indeed be obtained, by up to a factor of two for $x \approx 0.004$ for valence quarks.

3. Charged-current Drell–Yan at high transverse mass

Drell–Yan measurements at the LHC are usually performed at the resonance peak, especially in the charged current channel. However, going off-peak considerably opens up the (x, Q^2) accessible range, where $Q = m_{\ell\ell}$ (neutral current) or $Q = m_{\ell\nu}$ (charged current). In particular, the high Q^2 region is especially interesting, given its sensitivity to physics beyond the SM (which can be studied in an effective field theory framework) and high-x anti-quark PDFs. Since neutrinos escape the experiment undetected, $m_{\ell\nu}$ is not experimentally accessible and the transverse mass, $m_{\mathrm{T}}^W = \sqrt{2 p_{\mathrm{T}}^{\ell} p_{\mathrm{T}}^{\nu} (1 - \cos\Delta\phi(\ell, \nu))}$, is used instead (see Figure 2 left), where the missing transverse energy E_T^{miss} is used as an experimental proxy for p_{T}^{ν}.

The results presented in Ref. [3] use the full Run-2 dataset (2015–2018, corresponding to an integrated luminosity of $140\,\mathrm{fb}^{-1}$). Both the electron and muon channels are analysed, while the $W \to \tau\nu$ process is treated as background. The fiducial region is defined using Born-level kinematics: $p_{\mathrm{T}}^{\ell} > 65\,\mathrm{GeV}$, $|\eta| < 2.4$, $200 \le m_{\mathrm{T}}^W \le 5000\,\mathrm{GeV}$ (2D: $m_{\mathrm{T}}^W \le 2000\,\mathrm{GeV}$), and $p_{\mathrm{T}}^{\nu} > 85\,\mathrm{GeV}$. Iterative Bayesian unfolding is used to report results in terms of Born or "dressed" particle kinematics, starting from the reconstructed quantities.

A crucial component of the analysis, given the non-resonant nature of the signal, is an accurate background estimation. Dedicated validation regions are defined, each targetting a specific background. For top quark production, which is estimated using simulation, an $e\mu$ region is defined. For

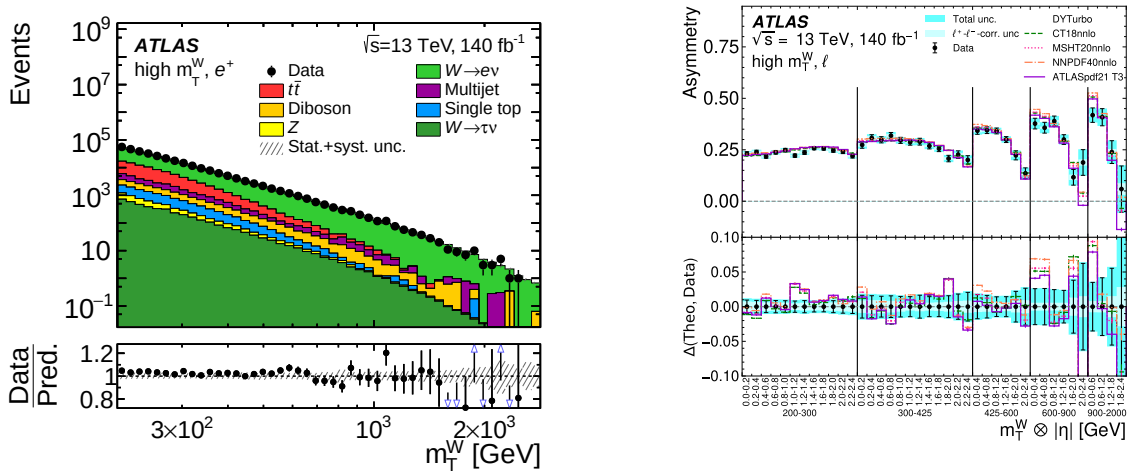

Figure 2: Left: transverse mass distribution in the positron channel. Right: charge asymmetry as functions of the transverse mass and lepton pseudorapidity, compared to predictions from various PDFs. Figures from Ref. [3].

the multijet background (data-driven, using the so-called matrix method), we remove the transverse mass selection, and veto events with $E_{\mathrm{T}}^{\mathrm{miss}} < 65\,\mathrm{GeV}$, which is characteristic of the Drell–Yan process. In all validation regions, a good agreement is found between the data and the predictions, validating the methodology.

The dominant source of systematic uncertainty is the electron energy or muon momentum scale. In the electron channel, uncertainties in the fake efficiency estimate for the multijet background also make a significant contribution to the uncertainty.

Measured cross sections span more than seven orders of magnitude. Over this impressive range, a good agreement is found between the data and predictions from Powheg+Pythia or Sherpa. Predictions from Powheg+Pythia are computed at next-to-leading order (NLO) in QCD, QED final-state radiation is modelled using Photos++, and mass-dependent k-factors are applied to correct to NNLO in QCD and NLO in electroweak (EW). Alternative predictions from Sherpa are computed at NLO in QCD for up to two additional partons (and leading order up to five additional partons), including NLO EW corrections, and also scaled up to NNLO QCD using k-factors. Charged-current Drell–Yan cross sections are reported as functions of the transverse mass and lepton pseudorapidity, in one or two dimensions, as well as the flavour asymmetry $\mathrm{d}\sigma(e^{\pm})/\mathrm{d}\sigma(\mu^{\pm})$ and the charge asymmetry (see Figure 2 right).

The results are used to constrain effective theory operators, in the context of the Standard Model effective field theory (SMEFT):

$$\mathcal{L}_{\mathrm{SMEFT}} = \mathcal{L}_{\mathrm{SM}} + \sum_i \frac{c_i^{(d)}}{\Lambda^{d-4}} O_i^{(d)},$$

where $d > 4$ is the dimension of the new operator and Λ is the energy cutoff scale. The four relevant dimension-6 operators, in the Warsaw basis, are $O_{lq}^{(3)}$, $O_{ll}^{(1)}$, $O_{Hl}^{(3)}$, and $O_{Hq}^{(3)}$. The world-best limits are set on the Wilson coefficient $c_{lq}^{(3)}$ (see Figure 3).

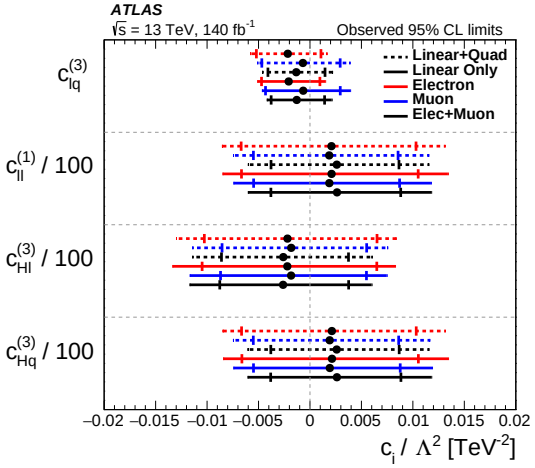

Figure 3: Observed limits on the Wilson coefficients for four SMEFT operators. Figure from Ref. [3].

4. High-mass Drell–Yan to $\tau\tau$

The ATLAS Collaboration has published the first measurement of inclusive $\tau^+\tau^-$ production as a function of the invariant mass $m_{\tau\tau}$ of the two τ-leptons [4]. Historically, the study of the neutral-current Drell–Yan process has lead to the discovery of many new resonances, such as the J/ψ and Υ mesons and the Z boson. The τ channel is of particular interest since many models predict enhanced couplings to third-generation fermions, such as in some supersymmetry or leptoquark scenarios. In addition, the measurement is done in bins of the b-jet multiplicity, in order to enhance the sensitivity to physics beyond the Standard Model. Results use the full Run-2 dataset (years 2015–2018), with a total integrated luminosity of 140 fb^{-1}.

Experimentally, only the hadronic τ-lepton decays are used, which enhances the signal purity in the selected data sample. Leptonic decays are considered, but only used for validation purposes. The fiducial phase space requires two hadronically-decaying τ-leptons with visible decay products such that ${p_{\mathrm{T}}}^{\ell} > 20$ GeV, $|\eta| < 2.47$, and ${p_{\mathrm{T}}}^{\tau} > 90(60)$ GeV for the leading (subleading) lepton. For b-jets, the selection is $p_{\mathrm{T}} > 25$ GeV and $|\eta| < 2.5$. Results are presented as a function of the visible mass $m_{\mathrm{vis}}^{\tau\tau}$. A particularity of this study is that this is an inclusive measurement: all processes contributing to this final state are considered as signal, which includes not only the Drell–Yan process but also the production of top quark pairs or multiple vector bosons, or the associated production of a top quark with a W boson (see Figure 4 left). Similarly to the other measurements presented here, results are unfolded to particle level using the iterative Bayesian method.

The measured cross sections are compared with SM predictions from Sherpa and Powheg+Pythia, both giving a good description of the data, as can be seen on Figure 4 (right). Limits on Wilson coefficients for fifteen SMEFT operators are also reported (Figure 5). The case of the $c_{\tau\gamma}$ coefficient is of particular interest, since the corresponding limits can be translated into limits on the τ-lepton anomalous magnetic moment a_τ, turning out to be a factor seven smaller than the ATLAS measurement in ultra-peripheral lead-lead collision [6] and competitive with the ones obtained by the CMS experiment using exclusive τ-lepton pair photoproduction, $\gamma\gamma \to \tau\tau$, in pp collisions [7]. Limits are also set on leptoquark and Z' models.

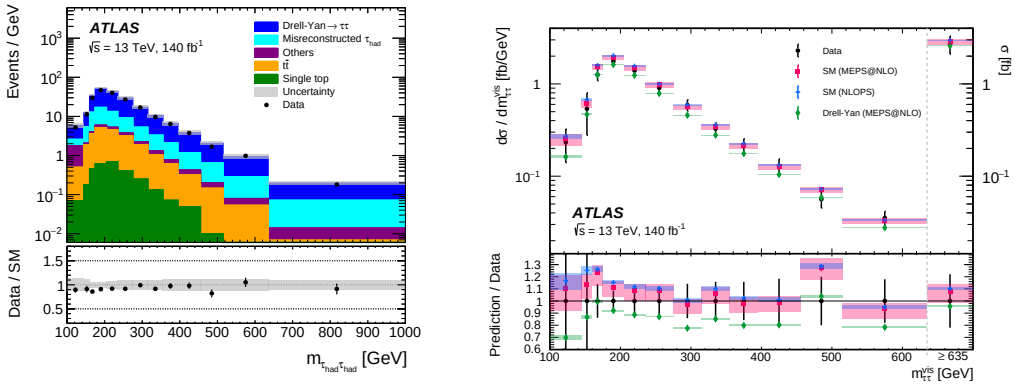

Figure 4: Left: comparison of the $m_{\tau\tau}$ spectrum in data with predictions for various processes. Right: unfolded cross section for inclusive $\tau^+\tau^-$ prediction, compared to predictions from SHERPA and POWHEG+PYTHIA. Figures from Ref. [4].

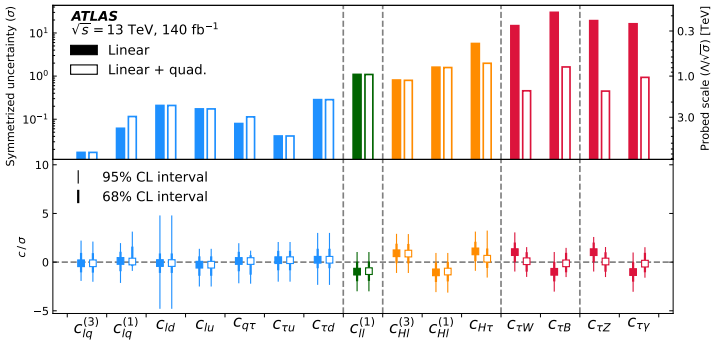

Figure 5: Limits on Wilson coefficients for fifteen SMEFT operators. Figure from Ref. [4].

5. Summary

We have presented three new measurements of the Drell–Yan process by the ATLAS experiment. Differential cross sections of W-boson production in low pile-up data [2] are more precise than the predictions, pointing to the potential constraining power of these data on quark PDFs. The first-ever measurement of the charged-current Drell–Yan process at high transverse masses [3] is also very interesting for quark PDFs, being again more precise than predictions, and provided the world-leading constraints on the Wilson coefficient $c_{lq}^{(3)}$. Finally, the first-ever measurement of $\tau^+\tau^-$ production at high masses [4] provides stringent constraints on SMEFT operators, as well as on leptoquark and Z' models.

References

[1] ATLAS Collaboration, "The ATLAS Experiment at the CERN Large Hadron Collider," JINST **3** (2008), S08003.

[2] ATLAS Collaboration, "Measurement of $W^{\pm}$-boson differential cross-sections in proton-proton collisions with low pile-up data at $\sqrt{s}$ = 5.02 TeV and 13 TeV with the ATLAS detector," Eur. Phys. J. C **85** (2025) no.7, 729.

[3] ATLAS Collaboration, "Measurement of double-differential charged-current Drell–Yan cross-sections at high transverse masses in pp collisions at $\sqrt{s}$ = 13 TeV with the ATLAS detector," JHEP **07** (2025), 026.

[4] ATLAS Collaboration, "A measurement of the high-mass $\tau\overline{\tau}$ production cross-section at $\sqrt{s}$ = 13 TeV with the ATLAS detector and constraints on new particles and couplings," JHEP **10** (2025), 054.

[5] ATLAS Collaboration, "Precise measurements of W- and Z-boson transverse momentum spectra with the ATLAS detector using pp collisions at $\sqrt{s}$ = 5.02 TeV and 13 TeV," Eur. Phys. J. C **84** (2024) no.10, 1126.

[6] ATLAS Collaboration, "Observation of the $\gamma\gamma \to \tau\tau$ process in Pb+Pb collisions and constraints on the τ-lepton anomalous magnetic moment with the ATLAS detector," Phys. Rev. Lett. **131** (2023) no.15, 151802.

[7] CMS Collaboration, "Observation of $\gamma\gamma \to \tau\tau$ in proton-proton collisions and limits on the anomalous electromagnetic moments of the τ lepton," Rept. Prog. Phys. **87** (2024) no.10, 107801.